ref: CERN/SPSC-2003-033
SPSC-M-707
23 October 2003

Status Report on Experiment NA48/2

The NA48/2 Collaboration:
Cambridge-CERN-Chicago-Dubna-Edinburgh-Evanston-
Ferrara-Firenze-
Mainz-Perugia-Pisa-Saclay-Siegen-Torino-Vienna

1 Introduction

A high precision study of charged kaon decays has been proposed using a novel design for simultaneous K^+/K^- beams and an upgraded NA48 set-up [1]. The main goal is to search for CP-violation in $K^\pm \to \pi^+\pi^-\pi^\pm$ decays. The experiment is designed to reach a sensitivity, limited by statistics rather than systematics, of $\sim 10^{-4}$ in the measurement of the direct CP-violating asymmetry

$$A_g = (g^+ - g^-)/(g^+ + g^-),$$

where g^+ and g^- are the slope parameters describing, respectively, the linear dependence of the K^+ and K^- decay probabilities on the u kinematic variable of the Dalitz plots. The u variable is related to the energy (E^*_π) of the *odd* pion (the pion having the sign opposite to that of the decaying kaon) in the kaon centre of mass system as follows:

$$u = (2M_K/m^2) \cdot (M_K/3 - E^*_\pi),$$

where M_K and m are the kaon and pion mass, respectively.

In order to achieve the required sensitivity, the experiment has to be carried out according to a strategy which ensures the highest possible immunity to detector asymmetries and perturbations. The approach followed consists in considering only slopes of ratios of u distributions which, alone or in suitable combinations that assure automatic compensation, can be distorted only by the simultaneous presence of time instability between data samples and Right-Left asymmetry in the detector acceptance.

Exploiting the high detection efficiency and precision in energy measurement for photons of the NA48 Liquid Krypton calorimeter (LKr), also the corresponding asymmetry A_g^0 in $K^\pm \to \pi^0\pi^0\pi^\pm$ decays will be measured, with a sensitivity again limited by statistics.

At the same time semileptonic decays of $K^\pm$ can be studied in order to measure the V_{us} element of the CKM matrix with better precision than currently available.

High statistics ($\sim 10^6$) of K_{e4} can be analyzed allowing the $\pi-\pi$ scattering length parameter a_0^0 to be measured with an accuracy of better than $1 \cdot 10^{-2}$. This permits the size of the $q\bar{q}$ condensate of the QCD vacuum postulated in χPT to be measured.

The present knowledge of several rare decays of the charged kaon such as:
$K^\pm \to \pi^\pm\pi^0\gamma$,
$K^\pm \to \pi^\pm\pi^0\gamma\gamma$,
$K^\pm \to \pi^\pm\pi^0 l^+l^-$,
$K^\pm \to \pi^\pm l^+l^-$,
$K^\pm \to l^\pm\nu l^+l^-$
and others, can be extended as well. This will allow χPT predictions at next-to-leading order to be tested.

The experiment NA48/2 [2] was approved by the CERN Research Board on November 23rd, 2000. Data taking started in 2003.

2 Simultaneous K^+/K^- beams

The new K12 beam line has been designed and built to transport simultaneously positive and negative particles with central momentum 60 GeV/c to the upgraded NA48/2 detector in the underground hall ECN3 at the SPS (fig. 1).

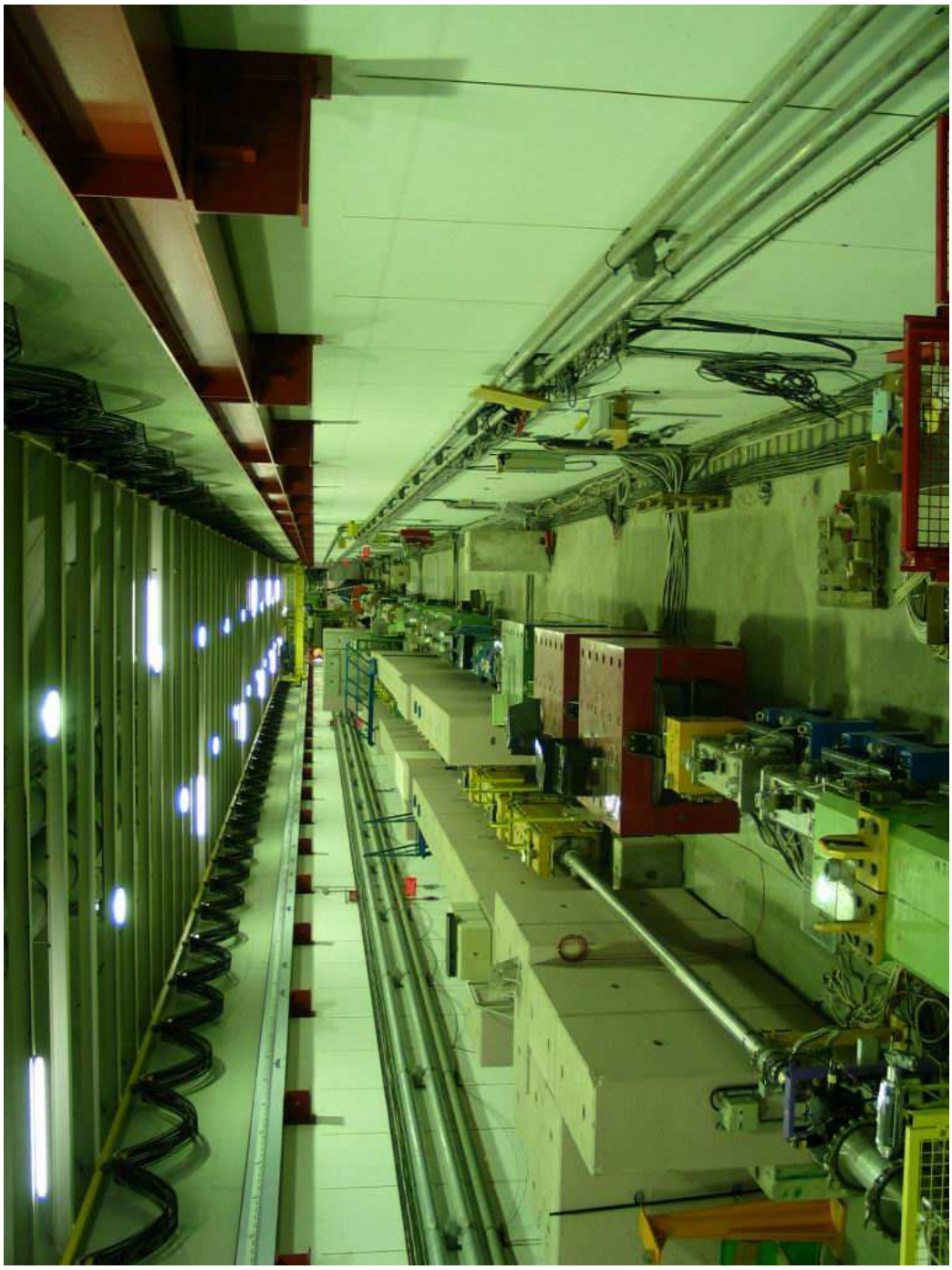

Fig. 1: The new K12 beam line built for experiment NA48/2.

The charged particles are produced in the target station T10 in TCC8 by 400 GeV/c primary protons - transported via the P42 beam line - at a chosen nominal intensity of $7 \cdot 10^{11}$ppp (with 16.8 s cycle time and 4.8 s flat-top)(fig. 2).

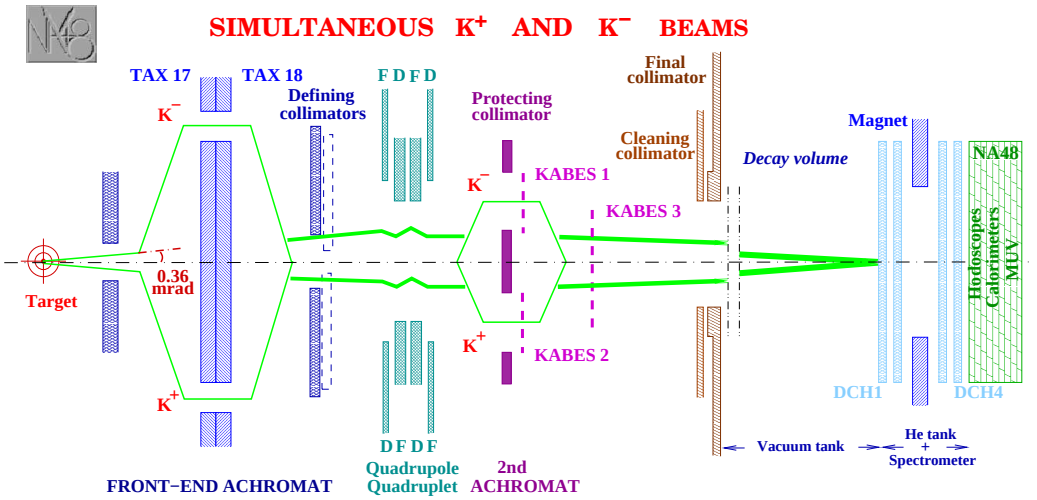

Fig. 2: Schematic vertical section of the simultaneous K^+ and K^- beam line (not to scale). Outside the dipole magnets the lower and upper envelopes respectively, of the K^+ and K^- beams are shown. Their axes are steered to coincide to a precision of ≤ 0.3 mm.

The two beams of opposite charge originating at zero degrees relative to the primary proton direction, each have an acceptance opening angle of ± 0.36 mrad in both planes, defined by a common collimator 24 m from the target. Upstream of this, the momentum band for the two charges is selected via a 'front-end achromat', consisting of 4 MTR-type dipole magnets with deflections in the vertical plane. The distribution of selected momenta for both charges has a width of $\pm 3.8\%$ (r.m.s.). A system of four alternating-gradient quadrupoles is designed to focus particles of each sign similarly in both planes. Rather than producing parallel beams of constant transverse extent as first proposed, we preferred to 'focus' both beams to similar, small 'spot' sizes (~ 5 *mm* r.m.s.) at the spectrometer position (shown in fig. 3), so as to minimize the transverse scale of any structure within the beam spots.

The angles of convergence of the beams remained small (mean ~ 0.04 mrad), leading to ≤ 1 mm transverse displacements over the length of the spectrometer. Any structure remaining inside the beam spots is naturally

exchanged between K^+ and K^- by regular inversions of all the beam ('achromat') polarities.

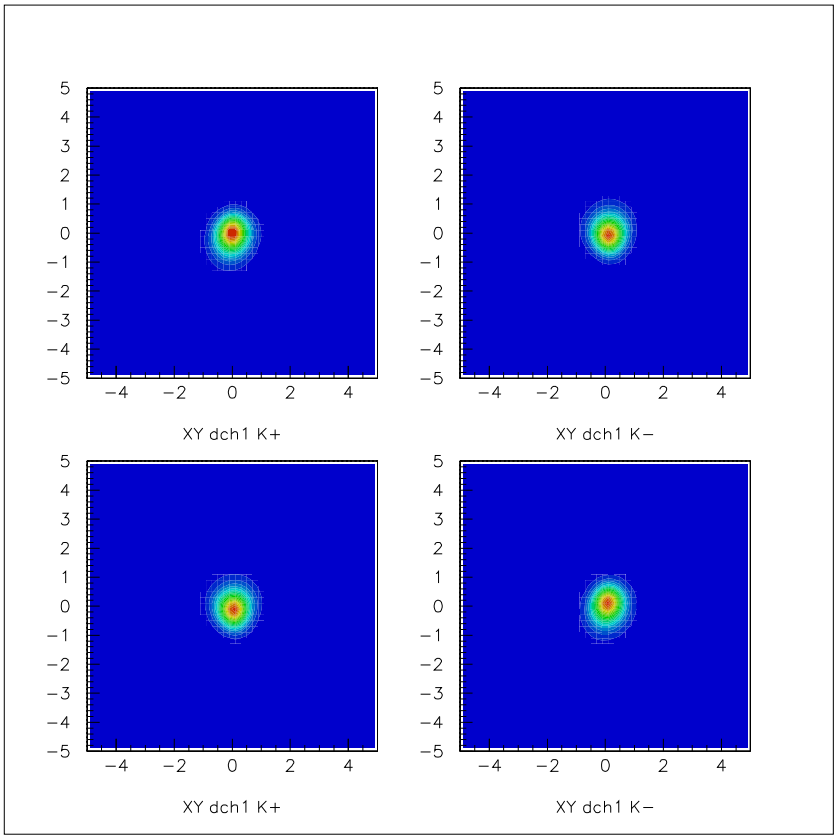

Fig. 3: The beam profiles at the plane of DCH1 reconstructed for K^+ selected by the lower path through the front-end achromat and K^- selected by the upper path through the achromat (upper plots), and corresponding plots with the paths through the achromat inverted(lower plots).

The positive beam flux at the exit of the final collimator was estimated to be $3.8 \cdot 10^7$ particles per pulse (of which $2.2 \cdot 10^6$ were K^+); the negative beam flux was $2.6 \cdot 10^7$ ppp ($1.3 \cdot 10^6 K^-$). The corresponding fluxes of positive and negative muons from K and π decays in the 114m decay volume were $1.1 \cdot 10^6$ and $0.8 \cdot 10^6$ per pulse, respectively. Using a series of magnetized-iron sweeping elements around the beam line upstream of the final collimator, the total flux of muons crossing the area ($\sim 5\ m^2$) of the detector around the central beam tube was limited to $\sim 1.5 \cdot 10^6$ per pulse.

These beams provided an adequate number of charged kaons ($(1.2 - 1.4) \cdot$

10^4 reconstructed $K^{\pm} \to (3\pi)^{\pm}$ decays per spill) at a level of muon background, which was predominantly due to pion and kaon decay downstream of the final collimator.

3 Set-up upgrade

In order to adapt the NA48 set-up, which was originally aimed at the detection of neutral kaon decays (mainly into two pions), to the study of charged kaon decays, especially into three pions, several elements were modified or upgraded. Fig. 4 shows a schematic view of the complete set-up. The

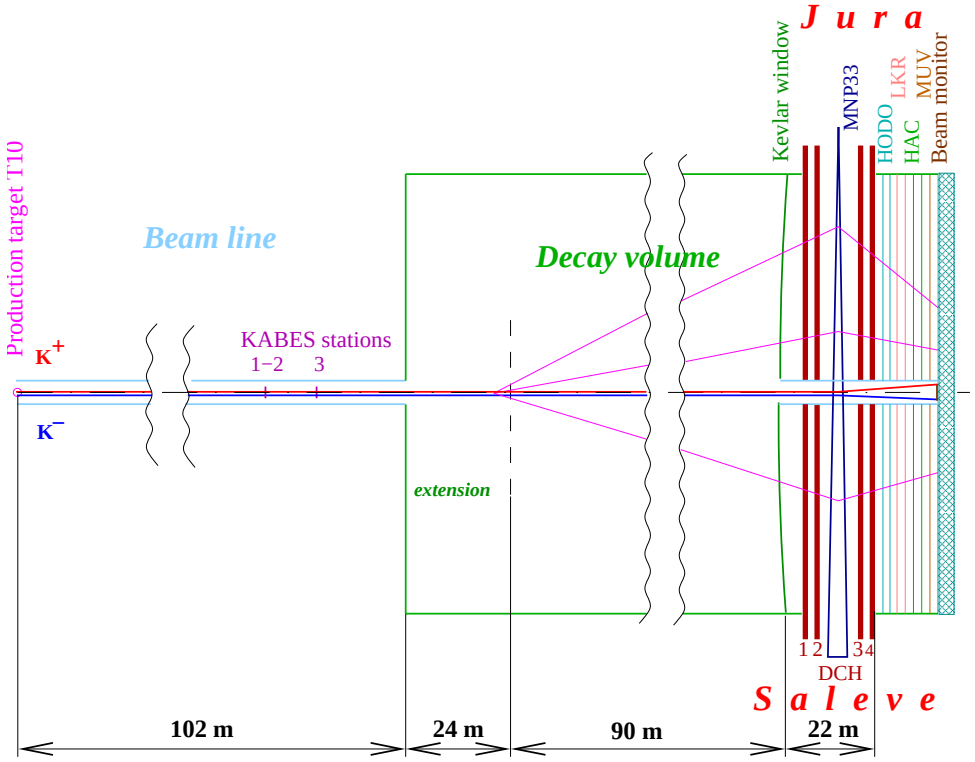

Fig. 4: Schematic top view of the upgraded NA48 Set-Up (not to scale).

decay vacuum tank was extended upstream by 24 m, allowing the acceptance for charged kaon decays to be increased by $\sim 30\%$. Measurements were made of a residual magnetic field in this part of the tank. Moreover, a set of Hall probes was installed to monitor the magnetic field inside the spectrometer magnet (MNP33).

A new beam detector, KABES (see Chapter 9), was integrated into the beam line to provide particle-by-particle momentum measurement. The final design and construction of KABES were completed after the successful beam test performed in 2002. KABES was installed as a complete sub-detector just before the 2003 run. Among the advantages brought by KABES are the resolution of the two-fold ambiguity in the kinematic reconstruction of K_{e4} decays and the possibility to reconstruct fully events from $K^{\pm} \to (3\pi)^{\pm}$ in which one of the pions escapes detection. It also enhances significantly the number of rare decay channels that can be investigated.

The third drift chamber (DCH3) of the magnetic spectrometer was fully instrumented with preamplifiers and read-out electronics (originally only two of four views were equipped with electronics). This allowed the efficiency of three particle decay reconstruction to be increased. In addition, the electronics of all drift chambers (DCH1-4) was reorganized in order to achieve left-right (*Jura-Saleve*) symmetry of possible read-out inefficiencies. Thus each of the electronics blocks was connected to read two, symmetrically placed groups of DCH wires.

The time stability of the beams and of the detector geometry is a major issue in NA48/2. In order to monitor on-line, and with high statistics, the geometry of the two charged beams, a dedicated detector, the beam monitor (see Chapter 10), was built and installed at the end of the experimental hall.

4 Trigger logics

The trigger setup for NA48/2 was prepared to be flexible, in order to cope with the new beam and their decay modes. The information available before the run was based on two short test runs performed in 2001 with a (single) charged beam (at different production angle) with a simpler muon sweeping, from which extrapolations to the 2003 running conditions were performed.

Possible pre-triggers and second level triggers were tested in 2001, mostly focusing on events with 3 charged tracks, including $K^{\pm} \to \pi^{\pm}\pi^{+}\pi^{-}$ and $K^{\pm}_{e4}$ decays. The conclusion was reached that with an improvement of the computing power of the charged trigger processor farm, a rather simple and unbiased pre-trigger requiring at least 2 tracks in the hodoscopes and no in-time signals in the ring anti-counters could be handled: in this way the use of potentially charge-asymmetric components such as hadron-calorimeter energy-thresholds and muon counter vetoes could be avoided safely.

The level 2 charged trigger processor farm ('massbox') was central to

the 2003 trigger. The farm asynchronously handles events triggered by the level 1 (pre-trigger) stage by analyzing the raw (uncalibrated) data from drift chambers 1, 2 and 4, and has a total time budget of 100 microseconds to take a decision. The basic algorithm in 2003 was based on the one used in the past for 4-track events: it looks for two compatible vertexes in the fiducial region, and is rather insensitive to imperfections of the spectrometer. This algorithm was complemented with a second one operating in cascade, looking for a single vertex with a reconstructed two-pion invariant mass compatible with the kinematic limit for 3π events. This combination of triggers had an overall inefficiency around 1%. The second component of the trigger allowed a fraction of events with 3 charged pions to be collected in which one of the pions goes undetected. These events are useful for systematic studies. It also allowed all three-track events (including $K^{\pm}_{e4}$ and $\pi^{\pm}l^{+}l^{-}$ decays) to be collected and was responsible for about half of the available readout bandwidth.

Triggers for events with a single charged track and photons in the final state, such as $K^{\pm} \to \pi^{\pm}\pi^{0}\pi^{0}$, exploited pre-triggers based on the detection of the electro-magnetic energy, for which the self-triggering level 2 pipelined neutral trigger chain was used. Little information was available from the 2001 test, and several alternative options were implemented, eventually leading to the choice of a peak-counting pre-trigger which gave the best combination of efficiency and rate . The fast extraction of the drift chamber data to the level 2 charged trigger farm was possible without overloading either the new chamber readout system or the upgraded trigger farm. The farm ran a different algorithm on this class of events, in which a loose missing mass cut is performed to reject the abundant $K^{\pm} \to \pi^{\pm}\pi^{0}$ decays, assuming the observed track to be that of a pion from the decay of a kaon of 60 GeV/c momentum along the beam axis. Such an algorithm is more sensitive to the detector parameters and geometry and good performance was obtained only after an internal calibration procedure of the on-line farm. This trigger accounted for another 25% of the available bandwidth.

The rest of the readout bandwidth was allocated to control triggers for the two above-mentioned channels. These included prescaled versions of the pre-triggers used, alternative independent selections and other special triggers designed for specific rare decay modes (such as K_{e2}). The latter were improved in the course of the run, while the main 3-track trigger was left unperturbed.

The commissioning of the trigger system was mainly performed during the first part of the run and some studies of non-rate-related effects continued

during the 25 ns run, reaching a baseline trigger configuration by the time the beam commissioning was completed. The allocation of trigger bandwidth always privileged the main 3-track trigger and its ancillary ones used to control its systematics.

The overall performance of the trigger in 2003 was satisfactory: the upgraded charged trigger farm was never saturated by the pre-triggers, even with somewhat more complex algorithms than used in the past. The efficiency of the 3-track trigger, monitored on line, was satisfactorily high and constant throughout the run (see fig. 5)

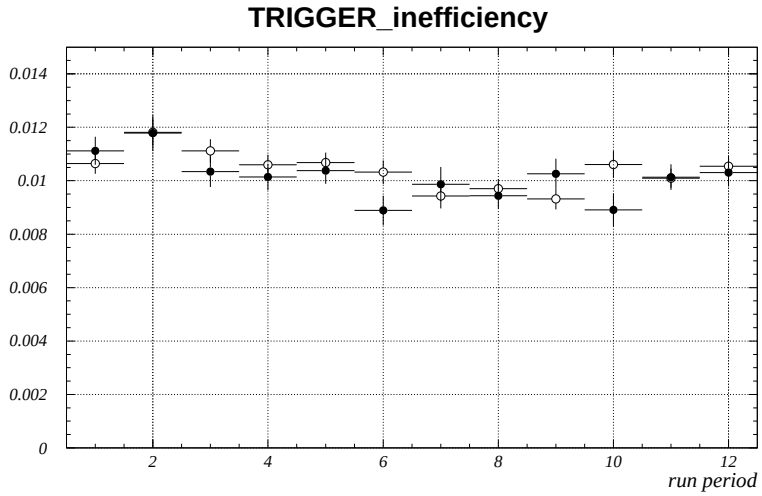

Fig. 5: The trigger inefficiencies for $K^+_{3\pi}$ decays (full circles) and $K^-_{3\pi}$ decays (open circles).

New algorithms for 1-track events were successfully used for the first time. An unexpected hardware failure of part of the neutral trigger chain led to the loss of a few days of 1-track triggers. During this time control and rare decay triggers were increased to saturate the bandwidth, thus allowing more systematic checks to be performed.

The level 1 trigger was smoothly interfaced to a second device, namely the new KABES detector. A new additional hardware interface was designed and built in order to allow maximum flexibility in the masking of level 1 triggers, so as not to saturate the KABES capabilities. All the relevant level 1 triggers were also sent to the KABES readout system, which was able to handle the required rate, thus allowing the KABES data to be present for

most classes of events. Random triggers proportional to beam intensity were also implemented, and for the first time used also as level 1 triggers in order to have KABES data available for software overlay.

The Level 3 software trigger ran in flagging mode since the beginning of the run, with a complete set of selection algorithms, allowing both a constant and fast monitoring of the data quality in the control room, and a quick and efficient way of selecting particular classes of events for further reprocessing.

5 Data taking

The main run of NA48/2 was scheduled from June 12 to September 8, corresponding to 88 days including $\sim$ 8 days of machine development. In addition, 5 days of standard proton beam were available in May, which were efficiently used to start the commissioning of the new beam during the preliminary tuning of the detector. An additional week in May with 25 ns r.f. beam structure was of little use for tuning the apparatus. The first ten days of running were devoted to understanding and tuning the new beams, to analyzing the recorded data, investigating background conditions, optimizing triggers and to final tuning of all the apparatus.

Since June 22 the data taking proceeded under nominal conditions. In order to minimize systematic uncertainties related to the apparatus asymmetry and beam structure, the magnetic fields in the spectrometer and beam line magnets were alternated regularly. The spectrometer magnet current was alternated on a daily basis, and all the beam line magnets were cycled and inverted once per week during the machine development pauses. The latter frequency was chosen to minimize losses of data, since the procedure is rather long and requires subsequent retuning of the beams, which in any case needed to be done after the MD.

Thus a self-complete data set, called *a supersample*, was accumulated over a two-week period. The chosen cycle assumes normal stability of running conditions within these two-week periods. Unfortunately, there were many interruptions of the SPS, that affected a large part of the data, making it less efficient for the asymmetry analysis.

Two complete *supersamples* and a partial one have been accumulated under relatively stable conditions in the latter part of the run, from August 6

to September 7. The relevant statistics of raw $K^{\pm} \to (3\pi)^{\pm}$ decays reconstructed for these *supersamples* are presented in Table 1. In addition ~ 50 millions of $K^{\pm} \to \pi^{\pm}\pi^0\pi^0$ were reconstructed for the same *supersamples*. It

Magnet polarities		*Supersample*			Total
beam line	spectrometer	I	II	III	
$-$	$+$	154	166	38	358
$-$	$-$	150	58	76	284
$+$	$+$	127	162	50	339
$+$	$-$	130	142	60	332
Total		561	528	224	1313

Table 1: Number of raw $K^{\pm} \to (3\pi)^{\pm}$ decays, in millions. For the asymmetry analysis the effective statistics will be reduced due to acceptance related cuts. Additional losses might be introduced due to rejection of bursts with detector or electronics malfunction.

is not clear whether the sparse data accumulated before August 6 (an additional $\sim 70\%$) is useful for the asymmetry analysis, due to the presence of additional systematic uncertainties. It can be used, nevertheless, for rare decay studies.

Five special runs were carried out in order to measure the positioning of the DCH's and to adjust the beam line geometry to that of the spectrometer. Data with 'straight' muons (with the spectrometer magnet demagnetized) were collected in three runs in June, end of July and end of August. Two other runs were preformed in which positive and negative beams are directed into the spectrometer outside the beam pipe at symmetric positions ($\pm 20\ cm$ in the x-, y-, u-, and v- coordinates at DCH1).

The efficiency of data taking over the full running period is shown graphically in fig. 6. In total, more than 30 days were lost for data taking due to problems not under control of the Collaboration, the major causes of which were: absence of beam, cooling problems, and the after-effects of power cuts.

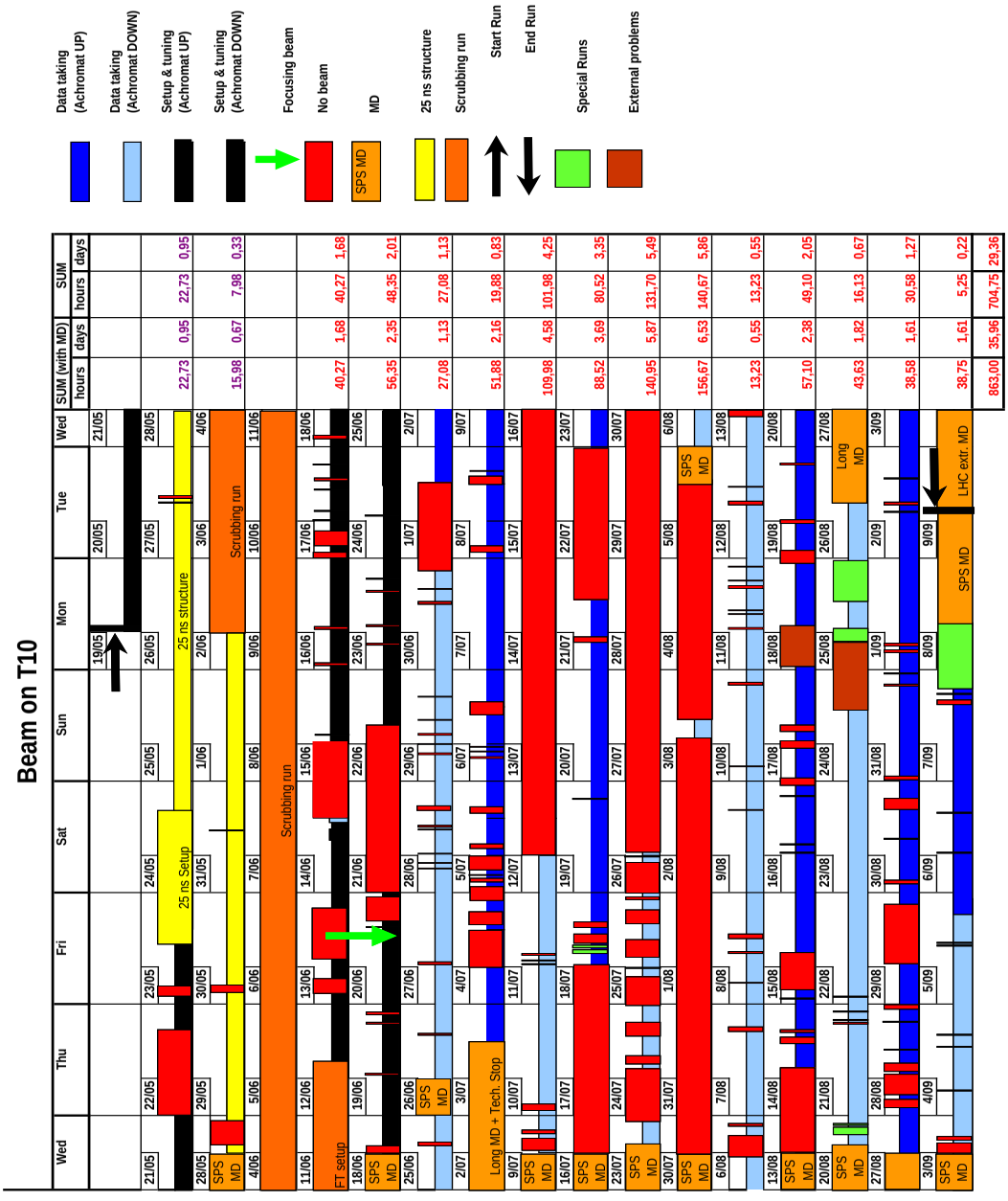

Fig. 6: Graphic of the availability of beam on T10 and the collection of the supersamples referred to in the text. The four left-hand columns list the time lost due to absence of the beam (including and not including MD)

6 Asymmetry measurement

As indicated in Chapter 1, the search for the CP-violating asymmetry, A_g, leads us to consider the ratios:

$$R(u) = constant \cdot (N^+(u)/N^-(u)),$$

where: $N^+(u)$ and $N^-(u)$ are the u spectra of $K^+ \to \pi^+\pi^+\pi^-$ and $K^- \to \pi^-\pi^-\pi^+$ decays, respectively, and the *constant* provides the normalization of $R(0) = 1$.
We may consider two such ratios:

$$R_S(u) = N^+(u)_U/N^-(u)_D$$

and

$$R_J(u) = N^+(u)_D/N^-(u)_U,$$

where the subscripts U and D indicate the direction of the field (*Up* and *Down*) in the spectrometer magnet. The subscripts S and J are chosen to indicate the direction of deflection of pions of the same charge as the kaon by the spectrometer magnet toward the *Saleve* and *Jura* sides. In case of perfect time stability these ratios would show a linear dependence on u. The corresponding slopes A_S, A_J, would be identical and, to first order, equal to Δg, which is related to A_g according to:

$$\Delta g = g^+ - g^- = 2g \cdot A_g,$$

where g is the average of g^+ and g^- ($g \simeq 0.2$ [8]).

It can easily be proved that:

- any Right-Left acceptance asymmetry which is stable between successive runs with U and D polarities of the magnetic field does not affect either A_S or A_J;
- a Right-Left symmetric change in acceptance during or between successive runs could affect both A_S and A_J but would be canceled when averaging A_S and A_J.

Thus a deviation from zero in the average of these slopes:

$$A = 0.5 \cdot (A_S + A_J)$$

would signal the CP-violating asymmetry, as long as the set-up is either *stable in time* or *symmetric*.

Each of the two other ratios:

$$R_U(u) = N^+(u)_U / N^-(u)_U$$

and

$$R_D(u) = N^+(u)_D / N^-(u)_D,$$

have slopes A_U and A_D which are equal to Δg as well, but only in case of Right-Left acceptance symmetry. However, the acceptance asymmetry cancels in their average, if this asymmetry is stable in time. So, the latter two ratios are more sensitive to systematic uncertainties and could be chosen to estimate these systematics in a conservative way. However, at this preliminary stage of the analysis the Collaboration considers it premature to show any number which could be ascribed to a real physics effect. Therefore, the above-mentioned slopes are shown with offsets applied to the scale.

Two additional ratios were considered:

$$R^+(u) = N^+(u)_U / N^+(u)_D$$

and

$$R^-(u) = N^-(u)_U / N^-(u)_D,$$

which do not contain information on A_g. The corresponding slopes A^+ and A^- are also sensitive to the Right-Left acceptance asymmetry, but their average ($A^\pm$) should be equal to zero, if the above conditions are fulfilled. Therefore all the distributions related to A^+ and A^- are shown without offsets.

All these slopes are biased only when an undetected asymmetric change in acceptance occurs during or between runs. This would change A_S and A_J with no coherent cancellation in their average and the same would happen for A_U, A_D, A^+ and A^-. To minimize the chance of such an occurrence:

- the functioning and efficiency of all detector elements have been monitored continuously and independently;
- the connections between the drift chamber and their readout cards have been arranged (see Chapter 3) so that any problem in a readout card would be reflected in the loss of efficiency in regions which are

symmetric with respect to the spectrometer axis, thus affecting A_U and A_D, or A^+ and A^- in a symmetric way;

- any residual asymmetry arising from slightly different geometry of the K^+ and K^- beams is reduced by alternating the beam line magnet polarities and averaging over the two beams passing through opposite paths in the achromat.

An express analysis has been performed using the statistics of *supersample I* to identify and roughly estimate the scale of major systematic uncertainties. Around 450 million $K^{\pm}_{3\pi}$ decays from the *supersample I* have been reprocessed for this analysis ($\sim$ 20% of the statistics were not processed for technical reasons). The 3π invariant mass spectra reconstructed for $K^+ \to \pi^+\pi^+\pi^-$ and $K^- \to \pi^-\pi^-\pi^+$ decays by implementing simple selection criteria (leaving $\sim$ 220 and $\sim$ 120 million $K^+_{3\pi}$ and $K^-_{3\pi}$ decays, respectively) are shown in fig.7 and indicate a negligible background level.

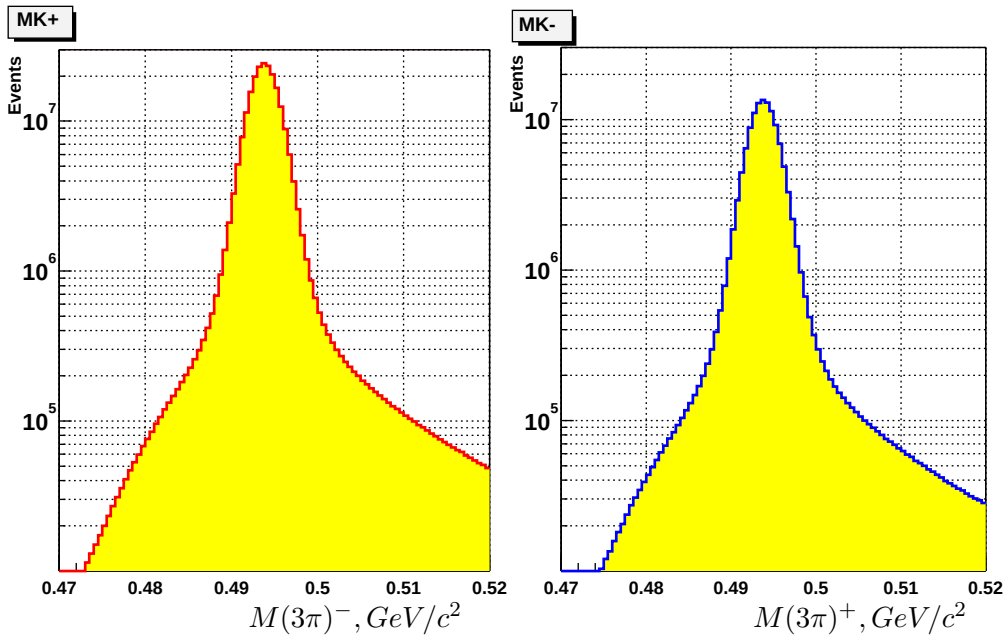

Fig. 7: The 3π invariant masses of reconstructed $K^+_{3\pi}$ (left) and $K^-_{3\pi}$ (right) decays.

The *supersample* was accumulated in 12 days of running, and each *day-sample* is recorded with alternating polarities of the magnetic field in the

spectrometer (*Up* or *Down*). The first 6 *day-samples* are recorded with the beam line magnet polarities such that positive particles pass through the upper path in the achromat, while the next 6 *day-samples* are recorded with the alternate configuration of beam line magnetic fields.

Fine calibration of the spectrometer magnetic field is done by adjusting the global momentum scale (at $\sim 10^{-3}$ level) for each *day-sample* separately, in such a way that the corresponding average value of the reconstructed K^+ and K^- masses is equal to the PDG value. In this way, the time stability between U and D *day-samples* is improved.

In fig. 8 the values of the reconstructed K^+ and K^- masses averaged over each pair of *day-samples* are shown. These values are obtained by Gaussian

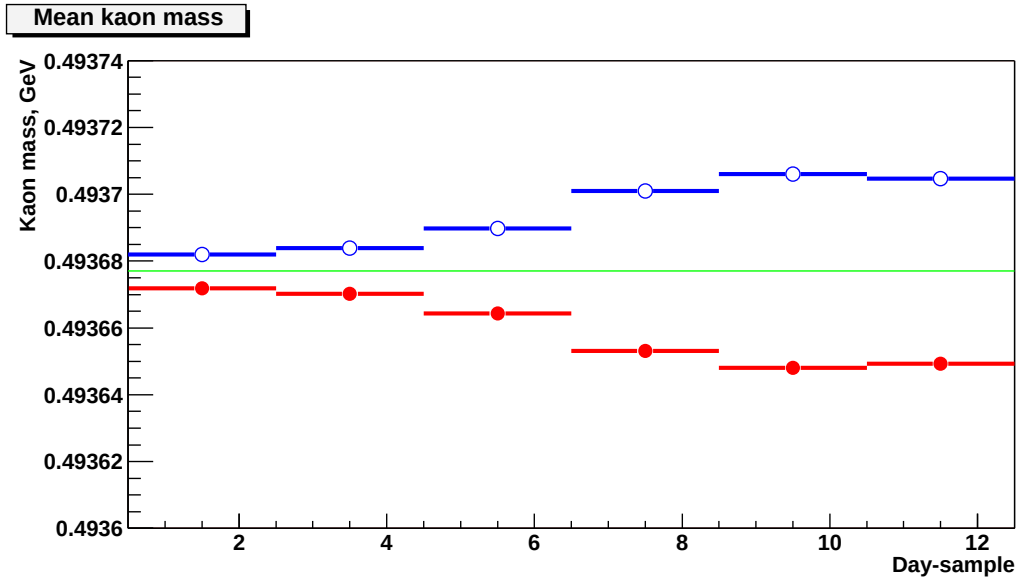

Fig. 8: The kaon masses reconstructed in different pairs of day-samples (red filled - circles K^+ or K^- deflected to the Saleve side and blue open circles - for K^+ or K^- deflected to the Jura side; green line - the PDG value).

fits to the corresponding 3π invariant mass distributions around the peak region. The data have been reprocessed with the position of the drift chambers adjusted to give equal K^+ and K^- masses for the first *day-sample*. The spectrometer magnetic field has *Up* polarity for odd *day-samples* and *Down* polarity for even *day-samples*. The mass subsequent differs between kaons deflected to the *Salave* side and the ones deflected to the *Jura* side as seen

in the plot. These differences are caused by gradual minute displacements of the DCH's along the x-axis. Somewhat surprisingly, such small time variations of the DCH alignment ($\sim 4\mu m$ per day) were detected and have to be corrected.

The impact of this misalignment on the measurements of the kaon masses and asymmetries have been estimated by introducing an artificial shift in the position of DCH4 along the x-axis. It has been shown that the $K^+_{3\pi}$ and $K^-_{3\pi}$ mass split of 70 KeV/c^2 could be induced by a DCH4 position shift of 50 μm. To reduce this Left-Right acceptance asymmetry and its variation with time, corrections to the pion momenta were introduced, corresponding to small shifts of DCH4 in each *day-sample*. The residual effect on the slopes is negligible.

Due to the presence of the beam pipe around the axis of the spectrometer, $K^\pm_{3\pi}$ decays are lost whenever the minimum distance of a pion from the axis is below ~ 11 cm. Since the acceptance as a function of u depends on this cut, additional selection criteria were applied. They reduce the acceptance asymmetry for positive and negative kaons caused by different relative positions of the beams and minimize any time variation of such differences. These criteria include radial cuts centered on the beam positions, defined by the centres of gravity (COG) for positive and negative kaon decay products separately in each momentum bin. They are applied at the planes of DCH1 (11.5 cm radial cut) and of DCH4 (13.5 cm radial cut). After these cuts ~ 170 million $K^+_{3\pi}$ decays and ~ 100 million $K^-_{3\pi}$ decays remain.

The u spectra ratios were measured independently in each of 10 kaon momentum bins to avoid differences related to a momentum dependence of the acceptance, partially caused by variations in beam position. A bin size of 1 GeV/c has been chosen taking into account the momentum resolution which is ~ 0.4 GeV/c.

To check possible residual systematic effects related to time variation and Left-Right acceptance on the asymmetry cancellation, the slopes A^+ and A^- obtained for the whole *supersample* in each momentum bin are shown in fig. 9(a). Their average (fig. 9b) integrated over all momentum bins is consistent with zero as expected:

$$< A^\pm >= (1.2 \pm 2.3) \cdot 10^{-4}.$$

The same statistics split over different achromat configurations (fig. 9(c) and 9(d)) shows small deviations from zero, which finally cancel.

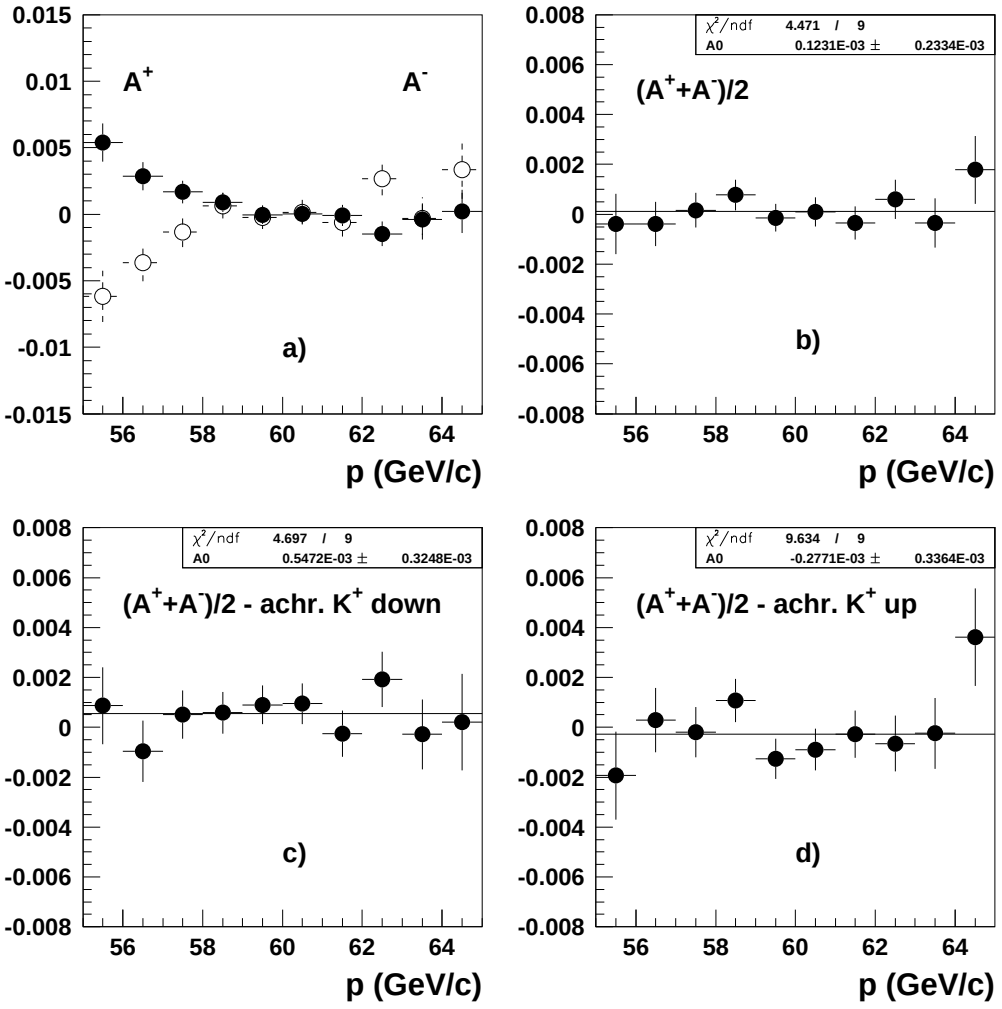

Fig. 9: The measured slopes A^+ (filled circles) and A^- (open circles)(a), and their average $A^\pm$ (b) at different kaon momenta. The average distribution split according to upper and lower paths through the achromats are shown in (c) and (d), respectively.

The corresponding plots obtained for A_S, A_J and A with similar selection criteria (fig. 10) do not indicate any Left-Right acceptance asymmetry or momentum dependent effects at a similar statistical level of $\pm 2.3 \cdot 10^{-4}$.

To check time stability integrated over all momentum bins the slopes A_S, A_J, and their average A obtained for the each couple of *day-samples* were compared with the value averaged over the whole *supersample*. The corresponding ratios (with offset) are plotted in fig. 11 and do not indicate significant variation in time.

We conclude that the Right-Left acceptance asymmetry is equalized for $K^+_{3\pi}$ and $K^-_{3\pi}$ decay, and is sufficiently stable in time within the *supersample* period.

Other possible systematic effects related to the residual magnetic field in the decay vacuum tank, accidental in time events and the DCH and trigger inefficiencies have been found to be less significant and do not affect the measured slopes at the present level of precision.

The possible major systematic uncertainties indicated in the proposal [2], as estimated on the basis of limited MC simulation, appear to be under control:

- the small non-collinearity of the beams is compensated by the analysis strategy chosen;
- the momentum binning effect is less significant than expected, since the beams were chosen to have a narrower momentum band than that indicated in the proposal.

We conclude that there are no uncontrolled effects visible in the data and that therefore possible residual systematic uncertainties do not exceed the statistical precision so far achieved.

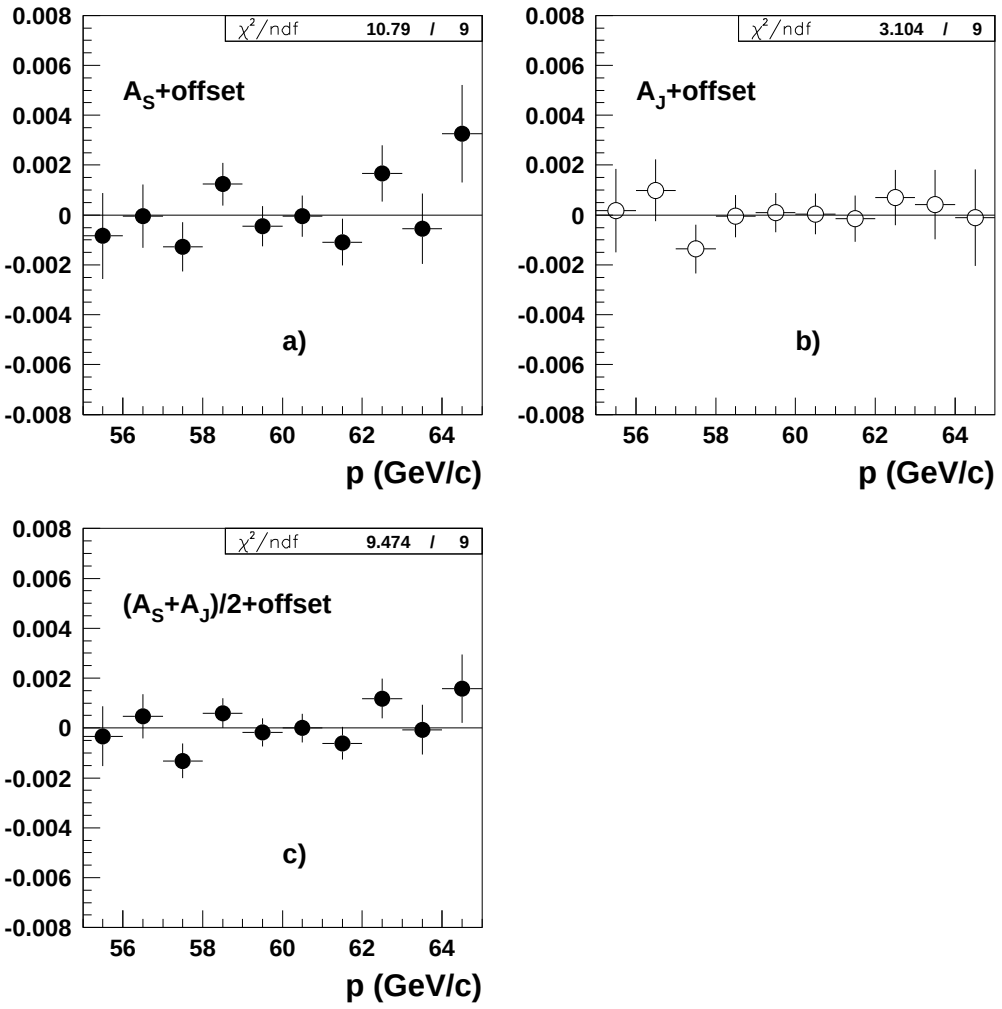

Fig. 10: The slopes measured at different kaon momenta: A_S (a), A_J (b), their average A (c), (all shown with an offset on the vertical scale) .

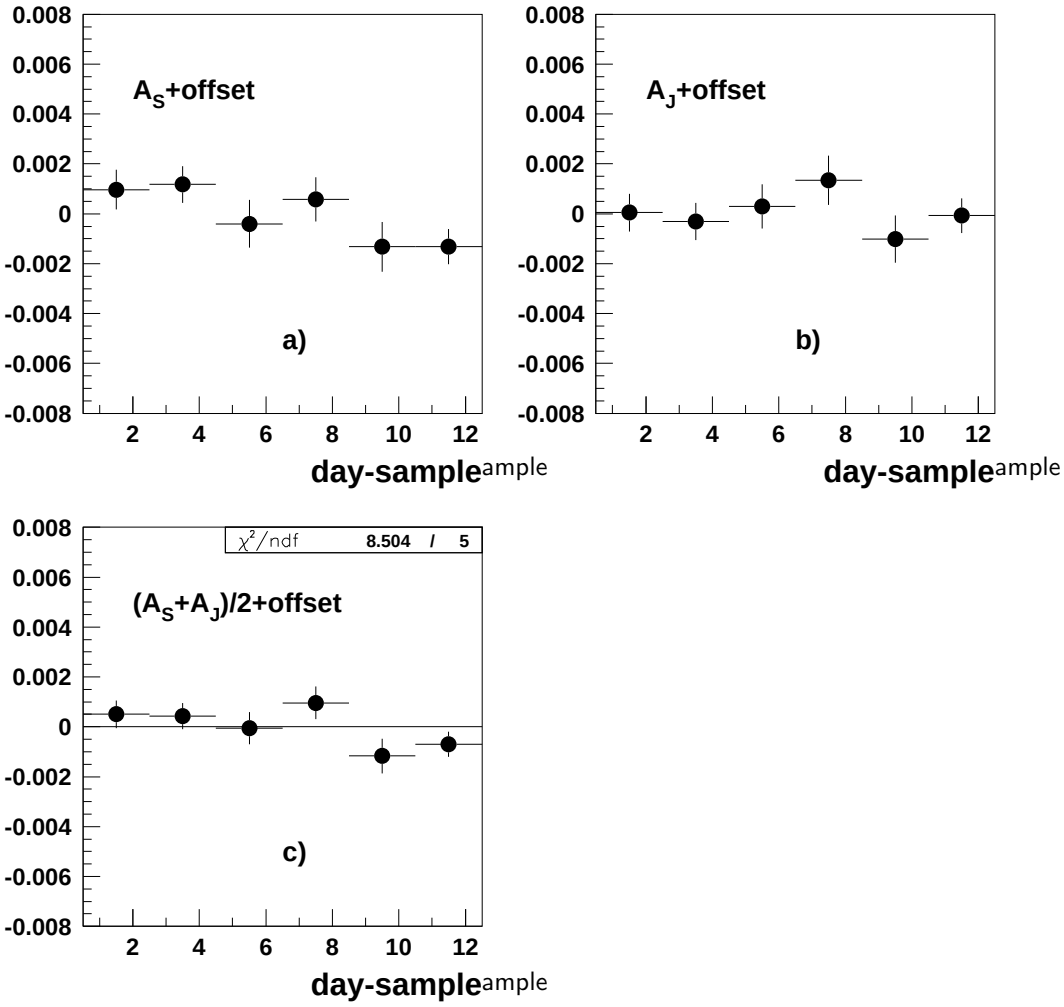

Fig. 11: The slopes A_S (a), A_J (b), and their average A (c) integrated over all momenta and measured independently in each couple of day-samples with opposite orientation of magnetic field relative to the overall average value (an offset is introduced on the vertical scales).

7 Rare decays

7.1 K_{e4}

To estimate the yield of K_{e4} events a test sample of 3748 bursts have been analyzed. The events were selected from the corresponding 3-track sample with additional selection criteria:

- one charged track is identified as an electron or positron candidate: the ratio of energy deposited in the LKr calorimeter to the associated track momentum should be $E/p \geq 0.9$.
- the $K_{3\pi}$ kinematic region in the plane $(M_{3\pi}, p_t(K, 3\pi))$ is excluded : an elliptical cut with half axes (10 MeV/c^2, 20 MeV/c) is applied.

To improve further the $e-\pi$ separation, a Neural Network (NN-method) was used, trained on pure pion and electron sample extracted from the data.

Two background sources arising from residual $e-\pi$ misidentification and/or extra electron production could be identified:

- $K^{\pm} \to \pi^+\pi^-\pi^{\pm}$ with one of the pions misidentified as an electron or positron. This represents $\sim 1\%$ of the K_{e4} events.
- $K^{\pm} \to \pi^{\pm}\pi^0$ followed by a Dalitz decay $\pi^0 \to e^+e^-\gamma$ and other modes producing π^0's also contribute $\sim 1\%$ of the K_{e4} events.

The distributions of the K_{e4} decay kinematic variables (Cabibbo Maksymowicz variables) are shown in fig. 12. The superimposed distributions from simulated events are in good agreement with the data. The 3π invariant mass and the reconstructed Kaon momentum distributions for the selected K_{e4} events are shown in fig. 13. Further studies should allow the background to be controlled to below the 1% level.

From this sample of 15807 events, the branching ratio was extracted to be $(3.87 \pm 0.2) \cdot 10^{-5}$, well compatible with the PDG value of $(4.08 \pm 0.09) \cdot 10^{-5}$.

In total, $\sim 7 \cdot 10^5$ K_{e4} events should be reconstructed from the data accumulated during the 2003 run.

7.2 Other rare decays

The accumulated samples of charged kaon rare decays: $K^{\pm} \to \pi^{\pm}e^+e^-$, $K^{\pm} \to \pi^{\pm}\mu^+\mu^-$, $K^{\pm} \to \pi^{\pm}\pi^0\gamma$, $K^{\pm} \to \pi^{\pm}\gamma\gamma$ will allow tests of next-to-leading order predictions of Chiral Perturbation Theory to be undertaken. As an example, a preliminary invariant mass spectrum with 1400

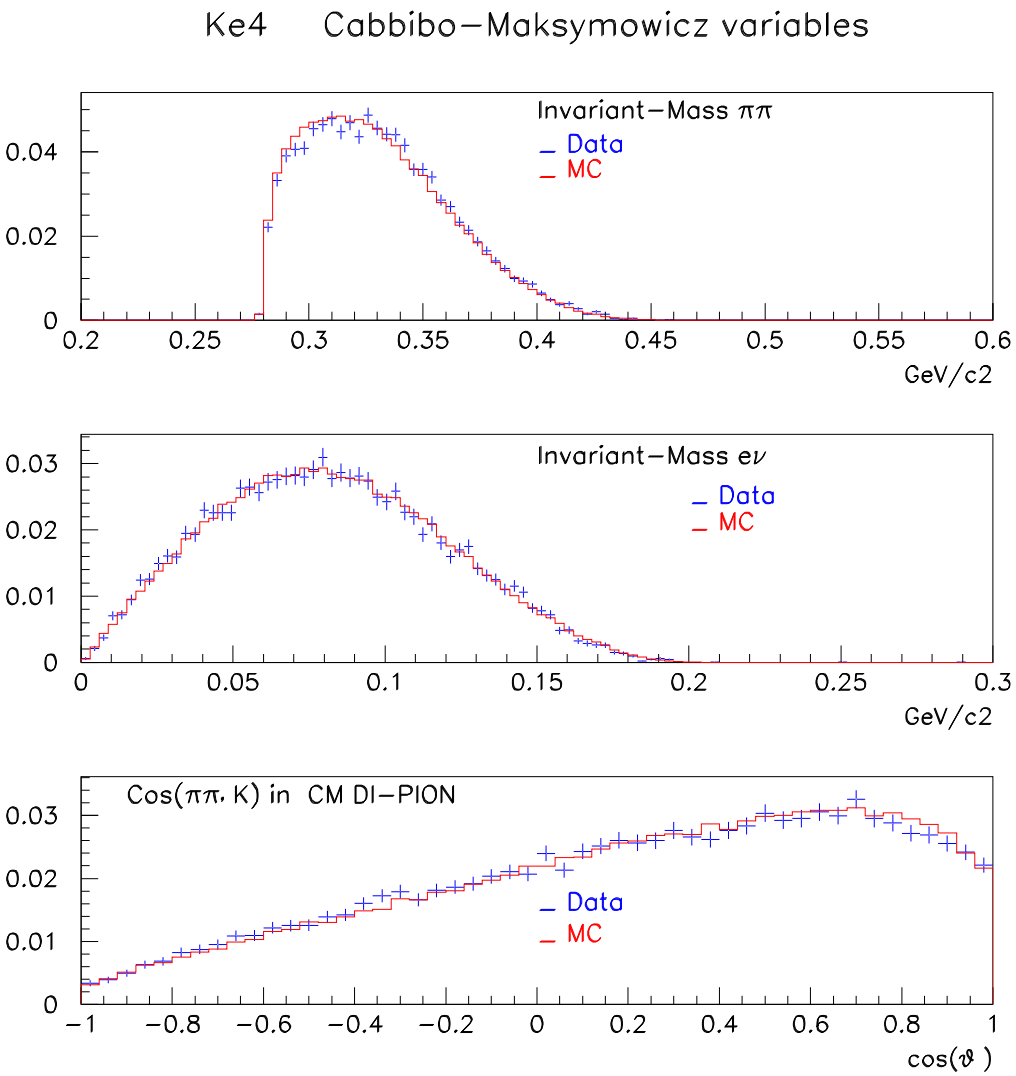

Fig. 12: Cabbibo Maksymowicz variables for data and simulated events.

good $K^{\pm} \to \pi^{\pm}e^{+}e^{-}$ events collected in one month of data taking (August, 6 – September, 7) is shown in fig. 14. By extrapolation to the total statistics collected during the 2003 run, it can be concluded that the total $K^{\pm} \to \pi^{\pm}e^{+}e^{-}$ sample amounts to about 3500 events.

High sensitivity studies and searches for the rare decays $K^{\pm} \to \pi^{\pm}\gamma l^{+}l^{-}$,

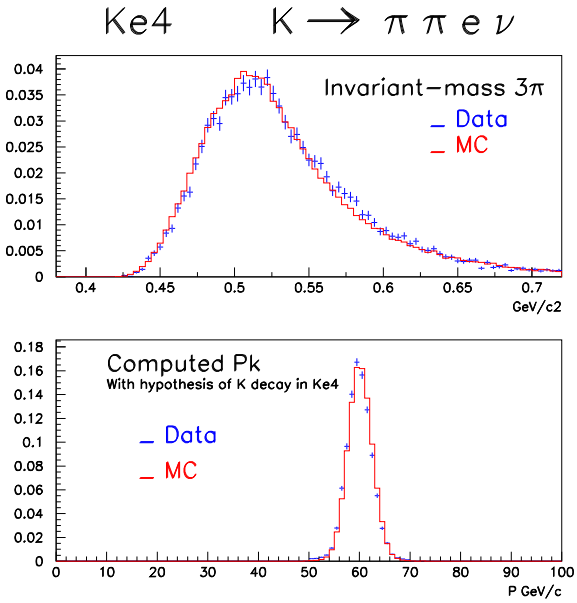

Fig. 13: Invariant 3 pion mass and reconstructed kaon momentum for K_{e4} selected events.

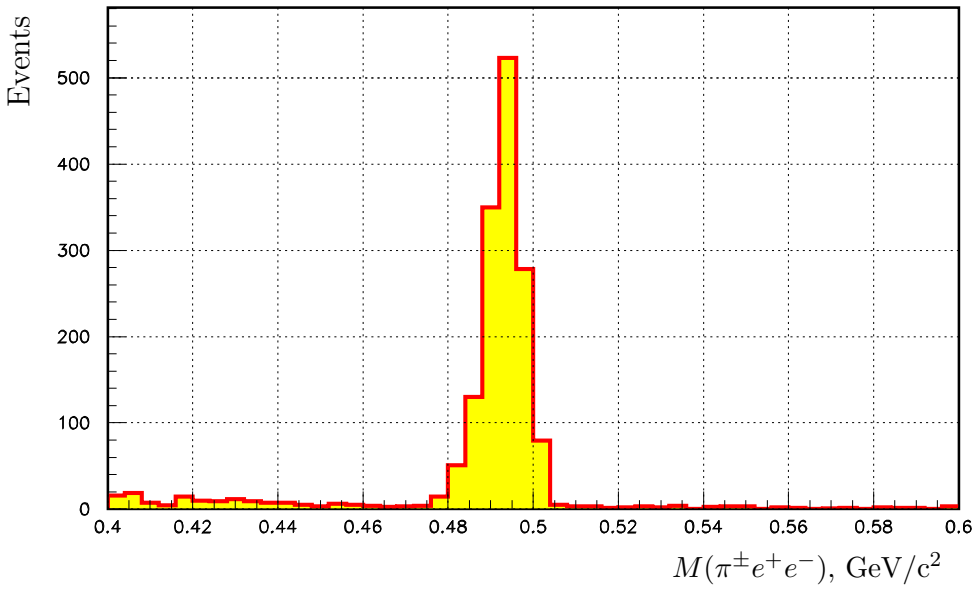

Fig. 14: $K^{\pm} \to \pi^{\pm}e^{+}e^{-}$ invariant mass spectrum obtained in one month of data taking.

$K^{\pm} \to \pi^{\pm}\gamma\gamma\gamma$, $K^{\pm} \to l\nu l^{+}l^{-}$, $\pi^{\pm} \to l\nu l^{+}l^{-}$ will also to be performed on the 2003 data.

8 Semileptonic decays

From the data taken in 2003, the NA48/2 experiment can make precise measurements of the branching ratios of the semileptonic decays and their normalization channels, whith as the ultimate goal, the determination of V_{us}. At present, V_{us} and V_{ud} are the most precisely known elements of the CKM matrix, with a fractional uncertainty at the level of $\sim 1\%$ and $\sim 0.1\%$, respectively. The magnitude of V_{ub} is such that its contribution to the unitarity relation $|V_{ud}|^2 + |V_{us}|^2 + |V_{ub}|^2 = 1$ can safely be neglected and the absolute uncertainties of the first two terms are comparable to each other. In other words, $|V_{ud}|$ and $|V_{us}|$ lead to two independent determinations of the Cabibbo angle, both at the 1% level. However, using the values quoted in [9], one finds a discrepancy between the two determinations at the two standard deviation level.

In fig. 15 we show a summary of all the available results on $f_+(0)V_{us}$, including the most recent results from the BNL-865 and KLOE experiments, where $f_+(q^2)$ is the form factor for K_{e3} decay. While the recent BNL-865 result disagrees with previous determinations of V_{us}, implying no deviation from the unitarity condition, the preliminary KLOE results agree with the previous data, thus confirming the potential problem. NA48/2 has the opportunity to clarify this long-standing puzzle.

In order to determine V_{us}, we need not only the branching ratio, but also the form factors. We plan to make precise measurements of both for the electron and the muon channels, $\mathrm{K}^{\pm} \to \pi^0 \mathrm{e}^{\pm}\nu_{\mathrm{e}}$, $\pi^0\mu^{\pm}\nu_{\mu}$.

The NA48/2 experiment will be able to perform these measurements from two different data samples: the first approach is based on Dalitz decays of the π^0 in order to use events with three tracks which are collected through the main 3π trigger, which is not downscaled, and has very high efficiency for the events of interest. Preliminary results show that we will have between $10^6 - 10^7$ events for each Dalitz decay mode, i.e. $\mathrm{K}^{\pm} \to \pi^{\pm}\pi^0_{\mathrm{D}}$, $\pi^0_{\mathrm{D}}\mathrm{e}^{\pm}\nu_{\mathrm{e}}$, $\pi^0_{\mathrm{D}}\mu^{\pm}\nu_{\mu}$, etc. . The second approach is based on data collected during a short, 8 hour (about 1900 bursts) dedicated run, which was performed during a period of unavailability of the normal trigger. The beam intensity was reduced to 1/8

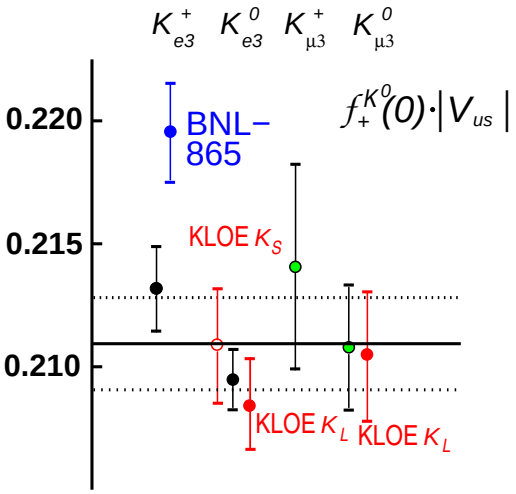

Fig. 15: Summary of $f_+(0)V_{us}$ results from K_{l3} decays of charged and neutral kaons.

of nominal and the trigger was based on a hodoscope signal for one or more tracks. Preliminary analysis shows a very clean sample, with all the main decay modes found to be consistent with expectation.

We have around 10^5 events for each semileptonic mode, $Ke3$ and $K\mu 3$, in this minimum bias run. This corresponds to several orders of magnitude more than for any single measurement available with $K^\pm$.

A signal of $K^\pm \to e^\pm \nu_e$ decays, based on the analysis of 1700 bursts, is clearly seen as a peak around zero in the distribution of missing mass squared (fig. 16). The background events, which are dominated by K_{e3} and π_{e2} decays (contributions from $K^\pm \to \pi^\pm + \pi^0$ and $K^\pm \to \pi^\pm + \pi^0_D$ are negligible), are well separated from the signal for both experimental data and simulated events.

Dedicated downscaled triggers for three-body semileptonic decays were also set up, which can provide an alternative approach for further checks of the results.

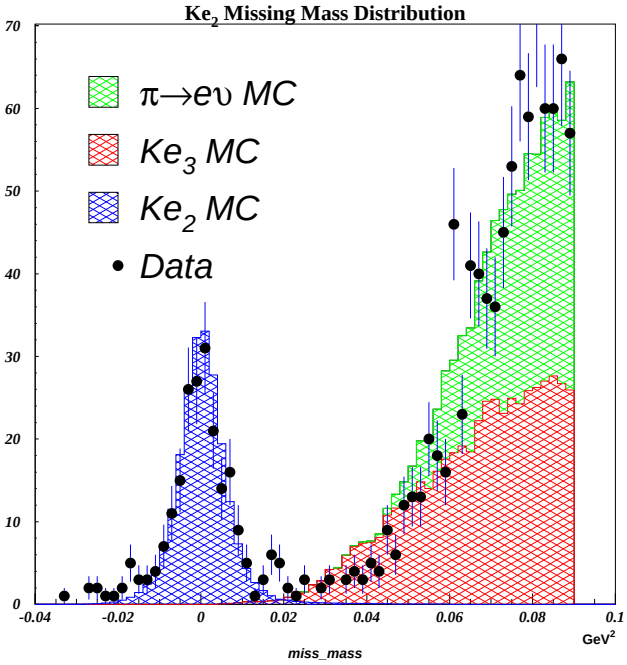

Fig. 16: $K^{\pm} \to e^{\pm}\nu_e$ selected from 1700 bursts.

9 Beam momentum measurement

KABES is a TPC-type detector using MICROMEGAS [3] with an amplification gap of $50\mu m$. The detector includes three double stations, each of them measuring the transverse coordinates and the time of the charged tracks. Two stations (one per beam) are located at the centre of a second achromat of 4 dipole magnets (sown in fig.2, at the position where the beams are separated and nearly parallel (fig. 17). The third one is installed on the beam line dwnstream of the second achromat where the beams are again collinear (fig. 2). This configuration of KABES stations allows the sign and the momentum of individual beam particles to be measured from the difference between vertical coordinates recorded in KABES-1/2 and in KABES-3.

The gas mixture, similar to that used by the COMPASS micromegas detector, i.e. $Ne(79\%) + C_2H_6(11\%) + CF_4(10\%)$, gives satisfactory performances for this application. The detector, after optimization, performed reliably up to twice the nominal flux of 6×10^7 particles per burst. The peak rate on the strips located in the centre of the beam was measured to be ~ 2

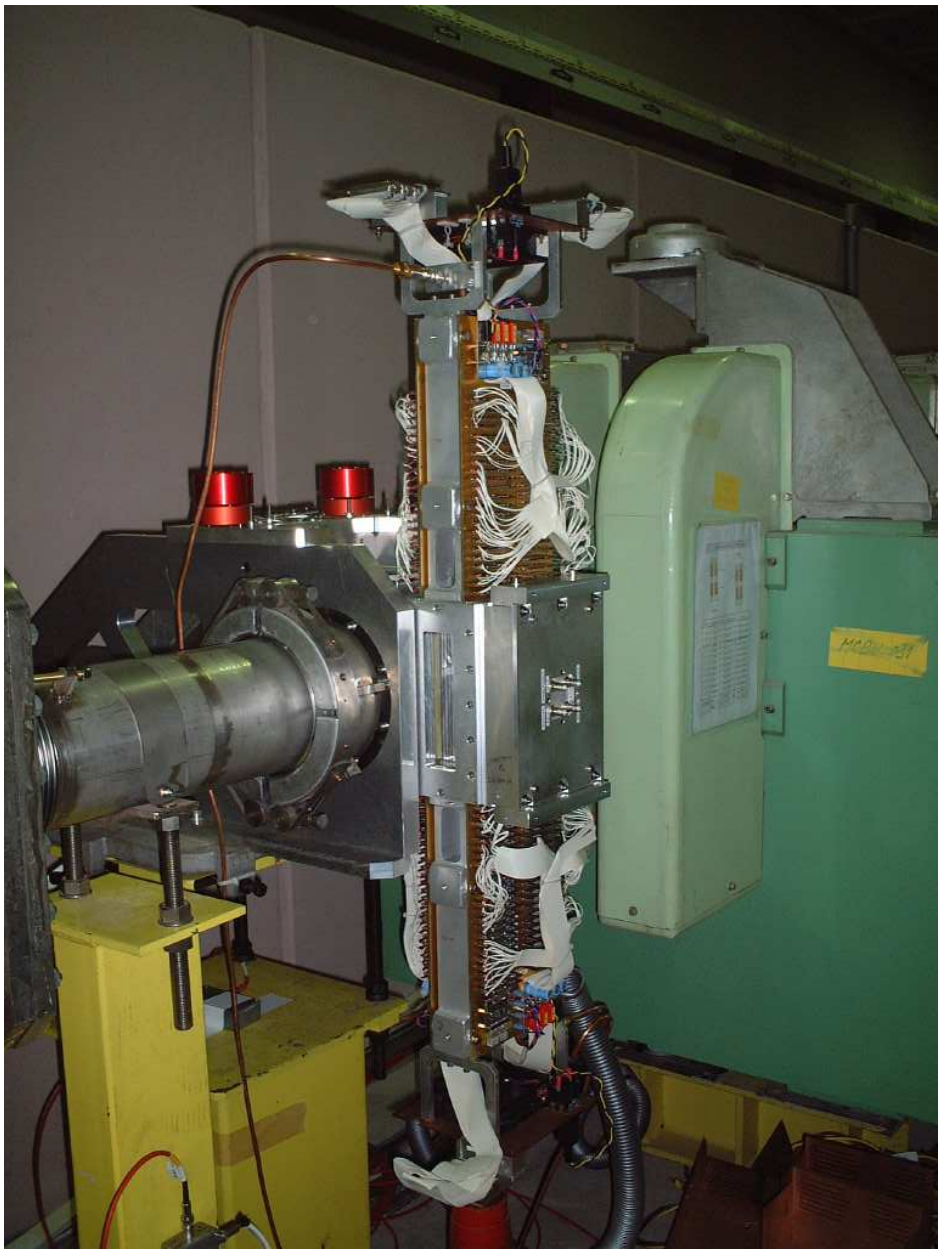

Fig. 17: The KABES-1/2 detector, which are moved horizontally by ~ 20 *cm outside the beam line to show the entrance window.*

MHz. As expected, a mean cluster size of 1.5 strips per particle track has been measured. The mechanics of KABES and the front-end preamplifiers and discriminators were designed and built in DAPNIA-Saclay.

The read-out electronics architecture is based on the HPTDC (High Performance TDC) chip developed at CERN [4]. The read-out is designed to work at an input rate up to 40 M hits/s with a maximum of 8 M hits/s on one strip, for a total rate of 960 MB/s per chamber. The read-out contains 288 TDC channels in total. The system is designed in VME standard. A 6U VME64x crate houses the main components: an interface module (SLVME) and the 6 read-out cards (ROCs). The operation of the system uses a standard desk-top PC, equipped with S-link to PCI cards and optical S-link interface. The capabilities of the ROC module are listed in table 2. The read-out modules of the system have been designed and manufactured in JINR-Dubna (fig. 18).

Characteristics	Units
VME-bus transfer rate	160 MB/s
Number of TDC channels	48 x 2
Time resolution measurement precision	86ps RMS
Max. hit rate per channel	8 Mhit/sec
Max. L1 trigger latency	5.5 μs
L1 trigger FIFO depth	16 events
Max. event size per ROC	1 KB (256 x 32bit)
L2 trigger Ring memory size /chamber	64 KB
Max. L2 trigger rate	25 KHz
Transmission TDC inputs standard	dECL

Table 2: ROC module main features.

At the nominal proton intensity of $7 \cdot 10^{11}$ ppp (corresponding to $3.8 \cdot 10^7$ particles per pulse) spatial resolutions of $\sim 100\mu m$ have been achieved in the horizontal drift direction (fig. 19) and of $\sim 130\mu m$ in the vertical direction using the strips (fig. 20). An excellent time resolution of 0.65 ns has been measured. This is essential to minimize the mistagging of an incident particle(fig.21)

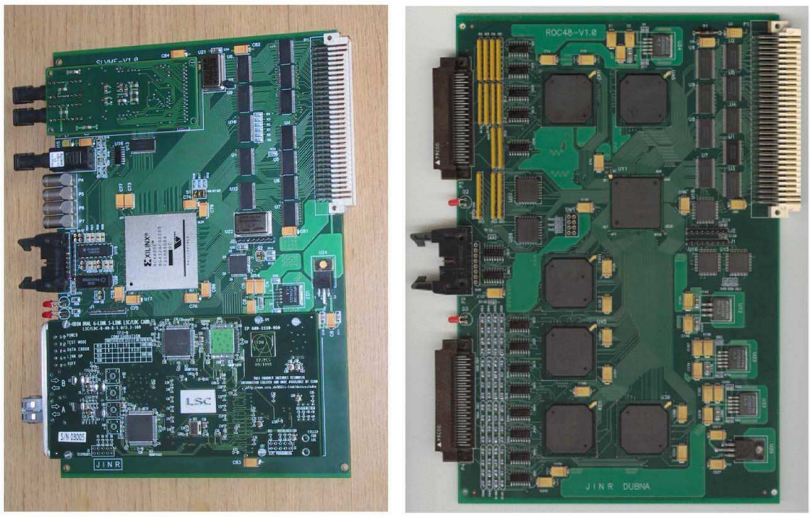

Fig. 18: SLVME and ROC modules.

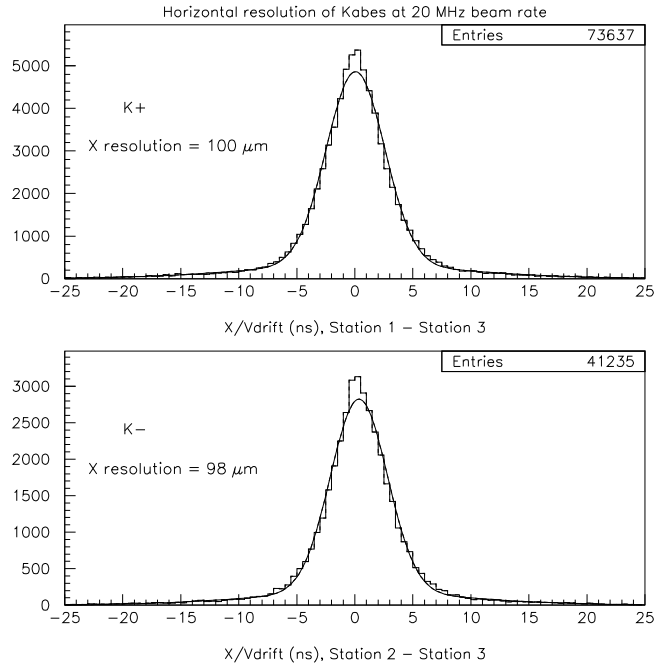

Fig. 19: The measured horizontal space resolution of KABES. The top plot is given for K^+, the bottom plot for K^-.

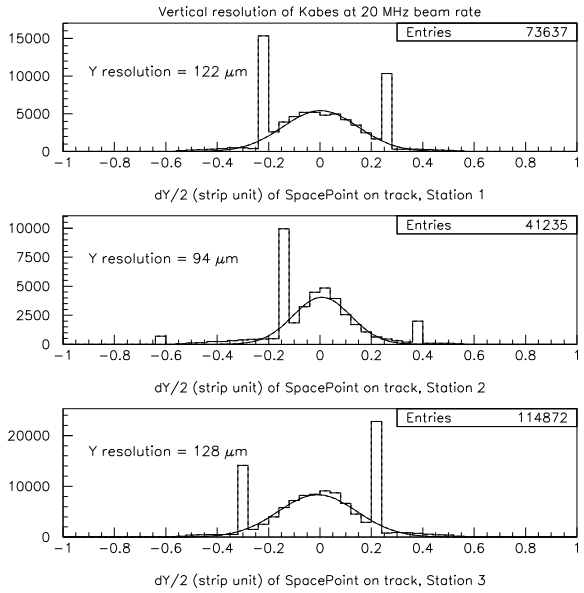

Fig. 20: The measured vertical space resolution of KABES. The spikes correspond to a cluster size of one strip in both cells of one detector.

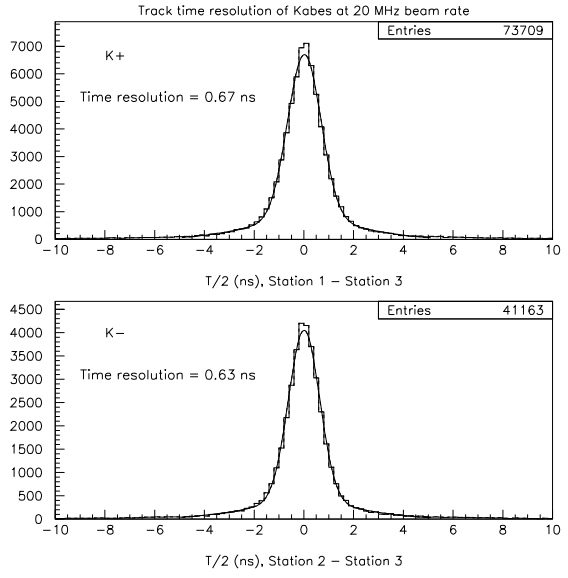

Fig. 21: The measured time resolution of KABES. The top plot is given for K^+, the bottom plot for K^-.

The pion momenta from $K^{\pm} \rightarrow (3\pi)^{\pm}$ decays are measured with the NA48 spectrometer. The resulting kaon momentum is compared to the $K^{\pm}$ momentum measured by KABES. The convolution of the resolutions of the two spectrometers is found to be 1.1% (fig. 22). From this number, the momentum resolution of KABES alone is inferred to be 0.8%. The same 3π event sample is used to control the mistagging level introduced by a charge or momentum mismatch, which is measured to be less than 5%. The fraction of events found without track at nominal proton intensity is less than 1%, which shows that the beam spectrometer system (KABES) is highly efficient.

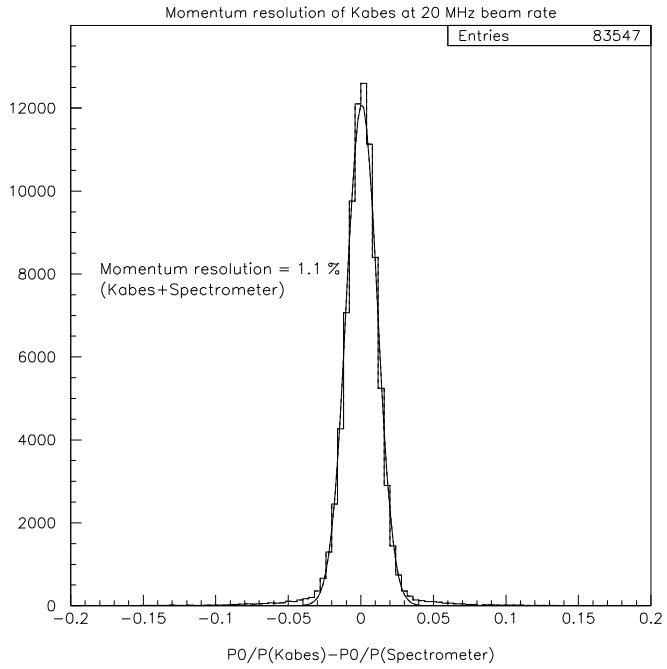

Fig. 22: The measured momentum resolution of KABES.

10 Beam position monitor

This monitor consists of two 8 x 8 matrices of scintillators, each 6x6 mm in the transverse direction and 9 mm thick for a total area of $\sim$ 50 x 50 mm^2 per matrix, wide enough to fully contain the beams (radial r.m.s. ~ 6 mm at the end of the hall). The scintillator blocks are separated by aluminium foils in

order to keep the optical cross talk to a minimum level. The two matrices are placed with their centres $\sim 100\ mm$ apart, corresponding to the separation of the two beams at the end of the beam line. The light from each matrix is collected by a flat face 8 x 8 pixel multi-anode PMT (Hamamatsu model H8500). Only the supply voltage between cathode and anode is tunable: it was kept at 800 V, corresponding to a gain of $\sim 1.5 \cdot 10^5$. Pixel gain non-uniformity is corrected by interfacing the scintillators to the PMT via a filter mask of 8 x 8 pixels; the transparency of each pixel is adjusted to compensate the gain of the respective PMT channel. The uniformity reached is better than 10%. The total (optical and electrical) cross-talk between adjacent pixels is measured to be at the few % level.

In the original design the 128 channels were read-out directly on the PMT backplanes. Eight daughter cards, housing 8 fast comparators each, were plugged on to the back of each PMT, via an interface mother card. The daughter cards received the PMT analogue signals via high impedance inputs and discriminated them with a common threshold. The output of the discriminators was sent to standard VME scalers, located $\sim 20\ m$ away. The high input impedance design avoided the need for amplification but had to be changed due to radiation damage to the integrated circuits. A new design was therefore adopted and implemented during the run, with the PMT signals transmitted trough twisted cables to the daughter cards located $\sim 70\ cm$ away from the beam pipe. In the last part of the data taking,with the new setup, no degradation of the PMT or the electronics was detected. The detectors were read digitally, recording the number of hits in each pixel in fast scalers. The readout of the scalers was performed 10 times per burst, in order to detect displacements of the beams within the burst.

The two scintillator and PMT systems could be moved horizontally (independently) and vertically (with a common displacement) by remotely controlled stepping motors (in steps of 0.001 mm).

High voltage scans were performed in order to fix a working point and to demonstrate that the measured geometry (centre of gravity and rms) of the beams was independent of the voltage above the working point. The chosen supply voltage when varied was 800 V, where the PMT signal was clearly above threshold (fixed at its minimum allowed value of 65 mV). At the maximum intensity some saturation phenomena were observed, due to a hardware limitation on the maximum value of the total anode current of 0.1 mA, which can be supplied by the PMT. It was shown that the beam geometry measurements were not affected by either saturation or increase of HV.

Position scans were performed by remotely moving the two detectors and comparing their changes in position with the measured displacement of the beams. Good linearity was found, with residual deviations compatible with the intrinsic burst-to-burst beam displacements (rms 0.05 mm). The detector is thus well suited to monitoring beam displacements with a resolution well below 0.1 mm.

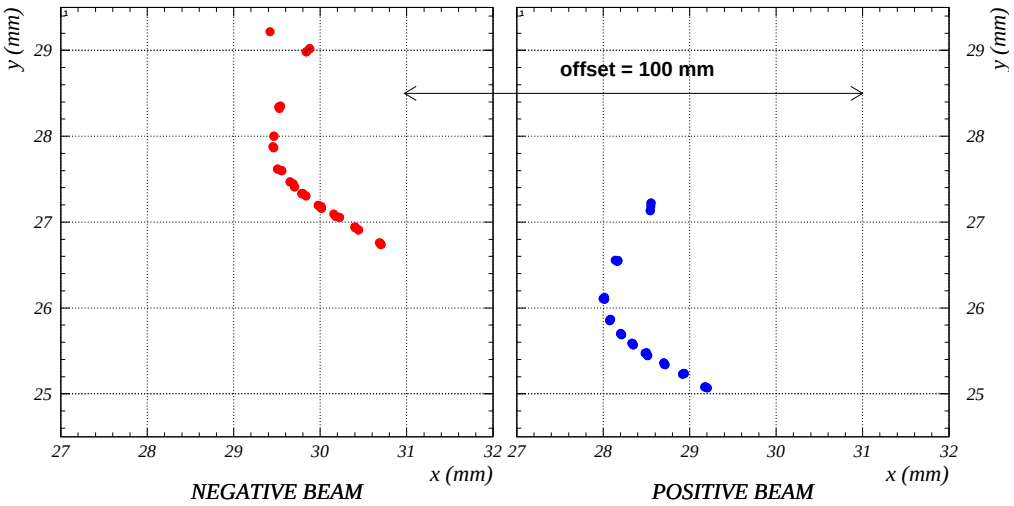

Fig. 23: The plot shows the centre of gravity (cog) of the positive and negative beams at the end of the hall, sampled ten times during the burst for each of three bursts. A common anti-clockwise displacement is evident. Errors are magnified by a factor of 10. The cog coordinates for the two beams are plotted with arbitrary off-sets; the actual distance between the two beams in the x direction is ~ 100 *mm.*

The new beam monitor served to detect of the displacements of the beams within the burst. Fig. 23 shows the displacement of the centre of gravity, separately for the positive and negative beams, sampled ten times during the burst. The data refer to three bursts, and the errors are magnified 10 times. The common displacement has its origin in the movement of the primary protons on the T10 target during the burst.

In future this monitor can be exploited to check the profiles of the beams on line to provide feed-back for their steering.

Summarizing, a new detector developed in a few months was successfully employed for the last period of data taking to measure with very high statistics the beam geometry, and in particular the beam displacements during the extraction.

In the future it could be exploited to check on-line the geometry of the beams and to ensure its stability through immediate feed-back on the steering.

11 Run in 2004

The proposal was based on the sensitivity that could be obtained with 120 days of data-taking at $1 \cdot 10^{12}$ 400 GeV/c protons per pulse onto target T10. Finally, due to the shortening of the scheduled, normal proton running time and the repeated interruptions of the SPS, only $\sim$ 50 days of main running time were available to NA48/2 in 2003.

According to a draft schedule of the SPS accelerator for 2004, $\sim$ 22 weeks (or $\sim$ 140 days, after subtraction of M.D. time) of proton physics might be available, not counting two special periods with 25 ns r.f. structure. NA48/2 would benefit from, and therefore requests, the major part of this time, preferably scheduled so as to minimize the length of planned interruptions. This would allow the experiment to be completed as approved, complementing the limited amount of data obtained in 2003. The conditions for data-taking, with due attention to some known details indicated below, have now been established and can confidently be predicted to allow NA48/2 to reach its announced goals of $\sim 10^{-4}$ precision on possible CP-violation and $\leq\sim 10^{-10}$ single-event-sensitivity to the decays of charged kaons.

The origins of some residual structure detected inside the focused beam spots can be addressed during the winter shut-down 2003-04. We would request that the alignment of the four beam-line focusing quadrupoles be checked and if necessary readjusted. A misalignment of $\sim$ 1 mm of one or more of these would explain the observed horizontal steering correction needed to bring the K^+ and K^- beams onto a common axis at the exit of the final collimator. Moreover, the pair of upstream horizontal steering magnets is also used to compensate the small deflections of the two beams by the stray field of the main muon sweeping magnets. A slightly off-axis passage of the beams through this stray field would explain a small correlation between the horizontal positions at the detector and the momentum of the $K^{\pm}$ ($dx/dp \sim \pm 0.3\ mm/GeV/c$). To correct for this as well as for any residual

quadrupole misalignment, this pair of steering magnets should be connected to separate power converters. We note that this (and any other) correlation is interchanged between K^+ and K^- by the regular inversion of all beam-line magnet ('achromat') polarities. Also, small variations of the mean K^+ and K^- momenta and of their common axis at the detector were observed during the 4.8 s SPS spill. These are attributed to ~ 0.3 mm movements of the mean position of the primary proton beam onto the 2 mm diameter production target (T10) and image similar movements on the upstream target T4. We would therefore request that such movements be minimized in the extracted proton beam line leading to T4. Finally, the main breaking of the symmetry between the K^+ and K^- beams in relation to the detector derives from the necessary, opposite horizontal deflections of the spectrometer magnet. The variations in the performance of the detector between consecutive periods of data taking with opposite polarity of the spectrometer magnet, when coupled to left-right asymmetries in the apparatus, have an influence on the asymmetry measurement in proportion to the typical duration of a run. Rather than inverting the current in the spectrometer magnet once per day, we plan to implement a procedure, by which this inversion can be performed on an hourly basis (with $\leq\sim 10\%$ loss of data-taking), thereby significantly reducing the effect of any time instabilities in the beam or the detector. We note that the feasibility of these improvements has been discussed whith the competent CERN specialists.

12 Summary

The experiment NA48/2 has been well prepared and the beam line, detector and triggers put into operation and tuned. The data accumulated in the 2003 run corresponds to only a part ($\sim 50\%$) of the planned statistics for the measurement of the direct CP-violating asymmetry in charged kaon decays.

A preliminary express analysis of a part of the 2003 run shows that the estimated statistical precision and systematic uncertainties of the measured asymmetry A_g are in agreement with those indicated in the proposal. The experiment can therefore benefit fully from a maximum possible complement of running time in 2004.

References

[1] J. R. Batley et al. Phys.Lett. B 544 (2002) 97.

[2] J. R. Batley et al, CERN/SPSC 2000-003, (2000);
NA48/2 status report (2001);
NA48 Status Report SPSC/M691, CERN/SPSC 2002-035 (3 November 2002).

[3] Y. Giomataris et al. NIM A 376 p29-35 (1996).

[4] M. Mota at al. A Flexible Multi-Channel High Resolution Time to Digital Converter ASIC. Nuclear science symposium, Lyon, France, October 2000.

[5] I. Mandjavidze, B.Vallage, NA48 Note: 02-01 (2002).

[6] L. Fausett. Fundamentals of Neural Networks: Architecture, Algorithms and Applications, Prentice-Hall, NJ, 1994.

[7] V. Kekelidze, NA48/2 status report, SPSC/M671, CERN/SPSC 2001-030 (20 October, 2001).

[8] K. Hagiwara *et al.*, Particle Data Group Phys. Rev. D **66** (2002) 010001.

[9] F.Gilman, K.Kleinknecht and B.Renk in: K.Hagiwara *et al.*, Phys.Rev. D **66** (2002) 010001-113.